

Juan Gabriel Segovia
Hernández*
Fernando Israel
Gómez-Castro
Eduardo Sánchez-Ramírez

Dynamic Performance of a Complex Distillation System to Separate a Five-Component Hydrocarbon Mixture

Distillation is one of the most used separation processes in chemical industry, although it is a highly energy-intensive operation. For multicomponent distillation, complex structures have been proposed in previous works, which may allow energy savings. Nevertheless, it is mandatory to understand the dynamic characteristics of such complex structures. In this work, the dynamic performance of a dividing-wall-based structure for the separation of a five-component mixture is studied. A sensitivity analysis is performed on the structure in terms of the interlinking streams, performing a singular value decomposition analysis to selected cases with different operational conditions. The designs with the lowest energy duties also showed the best open-loop properties.

Keywords: Complex distillation configuration, Dividing-wall columns, Multicomponent distillation

Received: May 28, 2018; *revised:* July 12, 2018; *accepted:* August 09, 2018

DOI: 10.1002/ceat.201800268

1 Introduction

Distillation is one of the most important and popular technologies for separation of multicomponent mixtures in chemical and petrochemical industries. Basically, in every production process, some of the chemicals go through at least one distillation column on their way from raw species to final product. Distillation is and will remain the separation method of choice in the chemical industry; by the year 2002, there were more than 40 000 columns in operation around the world [1]. However, high energy consumption and relatively low thermodynamic efficiency severely limit the development of distillation. Therefore, reducing the energy consumption is an urging motivation for studying distillation columns [2].

A survey conducted in the mid-1990s estimates that the energy input to distillation columns in the United States accounts for ~3% of the country's entire energy consumption [3]. It is clear that the efficiency of the separation can have a substantial influence on the profitability of a process; therefore, methods of improving the energy efficiency of distillation systems are constantly pursued. Thus, innovations toward energy-efficient distillation configurations for a given separation task traditionally have been of interest to the process industry. The volatility in energy prices in recent years has renewed interest in the synthesis, design, operation, and control of complex column configurations that can be significantly more energy-efficient than a conventional light-out-first (direct sequence) or heavy-out-first (indirect sequence) train of simple distillation columns [4].

One type of novel distillation systems for multicomponent separations is the dividing-wall column (DWC), which takes

the advantage of process intensification that reduce both the number of columns and the number of heat exchangers compared to conventional configurations. The DWCs for ternary separations have been widely studied, and many applications demonstrated that energy consumption can be reduced by 30–50% compared to conventional columns [5–7]. Remarkably, these DWC benefits are not limited to ternary separations alone, but they can be present also in azeotropic separations [8, 9], extractive distillation [8, 10], and reactive distillation [11, 12].

On top of that, the last decades witnessed major progress in design, modeling, simulation, control, optimization, and applications of DWCs, thus taking this technology to a certain higher level of maturity [13]. This idea is not limited only to three-component mixtures. According to Christiansen et al. [14], in general a DWC column is: “a column arrangement, separating three or more components using a single reboiler and a single condenser, in which any degree of separation (purity) can be obtained by increasing the number of stages, provided the reflux is above a certain minimum value and the separation is thermodynamically feasible.” As industrial separation problems very often involve four or more components, for such prob-

Prof. Juan Gabriel Segovia Hernández, Fernando Israel Gómez-Castro, Dr. Eduardo Sánchez-Ramírez
gsegovia@ugto.mx
Universidad de Guanajuato, Campus Guanajuato, División de Ciencias Naturales y Exactas, Departamento de Ingeniería Química, Noria Alta S/N Col. Noria Alta, 36050 Guanajuato, México.

lems, due to complexity it is necessary to study multicomponent DWCs.

Potential benefits of a DWC could become even larger if such a column could be used for obtaining four or more pure products or fractions from a feed containing respectively the same number or more components. For example, Blancarte-Palacios et al. [15] demonstrated that a quaternary DWC allows for reduction in energy consumption of 40 % in comparison with a conventional configuration. Also, Ge et al. [16] found that the DWC is energy-efficient compared to a conventional column sequence for multicomponent separation, which is used for olefin separation in fluidization methanol-to-propylene process.

On the other hand, a main reason for the slow acceptance of DWCs by the process industry was the fear of expected control-related problems. The control of a DWC is more difficult than that of a conventional scheme with two columns for the separation of ternary mixtures because there is more interaction among control loops. Besides, the absence of proper controllability could mean the absence of energy savings if the optimal operation is not accomplished [17–19]. In general, the economic potential of DWCs has already been recognized, but their control properties have not been studied to the same degree. Kaibel [20] reported that the control of DWCs corresponds to that of a conventional distillation column with a side product. This result has gained importance since thermally coupled distillation columns have been implemented successfully and operated in industrial practice [21].

Ling and Luyben [22] explored the use of temperatures to avoid expensive and high-maintenance composition analyzers in a DWC. Van Diggelen et al. [24] explored the DWC control issues and made a comparison of various control strategies based on PID loops. In the case of quaternary separations, some results have been described. For example, Cárdenas et al. [24] found that the theoretical control properties of a fully thermally coupled distillation sequence and a thermally coupled distillation sequence with two side columns were better than those of the uncoupled distillation sequence. This result was corroborated using dynamic simulations for different pairings in the control loops [25]. In general, those works have found the rather unexpected result that the control properties of the DWC were better than those of the conventional schemes in many cases, so that the predicted savings in both energy and capital would probably not be obtained at the expense of operational and control problems.

In this work, the dynamic performance of a complex five-component DWC system, previously reported by Caballero and Reyes-Labarta [26], is analyzed under different operating points, including the one with minimum energy consumption. The control analysis properties are evaluated with the application of the singular value decomposition technique. To the knowledge of the authors, there are only few works dealing with the dynamic properties of dividing-wall systems for the separation of mixtures with four or more components. Thus, this work will give insights about the dynamic performance of a complex dividing-wall system for the separation of a five-component mixture, which has been reported as an energy-saving approach in previous works [26].

2 Case Study

A five-component mixture was to be separated in a thermally coupled configuration. The mixture was composed by *n*-hexane, *n*-heptane, *n*-octane, *n*-nonane, and *n*-decane. Since it was a hydrocarbon mixture, vapor-liquid equilibrium can be modeled using the Chao-Seader equation. The feed mole composition ($x_{F,i}$) is presented in Tab. 1, together with the relative volatilities ($\alpha_{i,HK}$), referred to *n*-decane. The total feed flow rate is 200 kmol h⁻¹.

Table 1. Five-component mixture.

Component	Symbol	$x_{F,j}$	$\alpha_{j,HK}$
<i>n</i> -Hexane	nC6	0.1	17.5
<i>n</i> -Heptane	nC7	0.2	8.37
<i>n</i> -Octane	nC8	0.3	4.04
<i>n</i> -Nonane	nC9	0.3	1.99
<i>n</i> -Decane	nC10	0.1	1.00

The mixture was separated in an intensified distillation system, with two DWCs linked by interlinking streams *FV2* and *FL2*, and by side streams *SS1*, *SS2*, and *SS3*, as illustrated in Fig. 1 a. This structure has been previously presented by Caballero and Reyes-Labarta [26], obtaining savings of 10 % in total annual costs through this intensified system. To simulate and analyze such system in a virtual environment, the thermodynamically equivalent structure shown in Fig. 1 b was used. The desired purity for each product was 98 mol %.

3 Methodology

The separation of multicomponent mixtures by complex distillation columns may result as compared to simple columns in an important reduction of energy consumption. The selection of such complex configurations depends strongly on the separation problem, i.e., composition, thermal condition of the feed, specification of the products, and relative volatilities of the components. Therefore, the development of simple and efficient design algorithms for the determination of all relevant design parameters under pinch conditions in a complex distillation column, which takes into account all previously mentioned separation parameters, constitutes an important step towards the development of a reliable approach for the evaluation of different distillation sequence alternatives involving complex configurations [27].

3.1 Synthesis of the Case of Study

The synthesis methodology has been previously reported by Caballero and Reyes-Labarta [26]. In this sub-section, the method will be briefly explained. The proposal starts with basic sequences and excluding non-basic sequences. They named basic sequences, those alternatives which may separate *N* com-

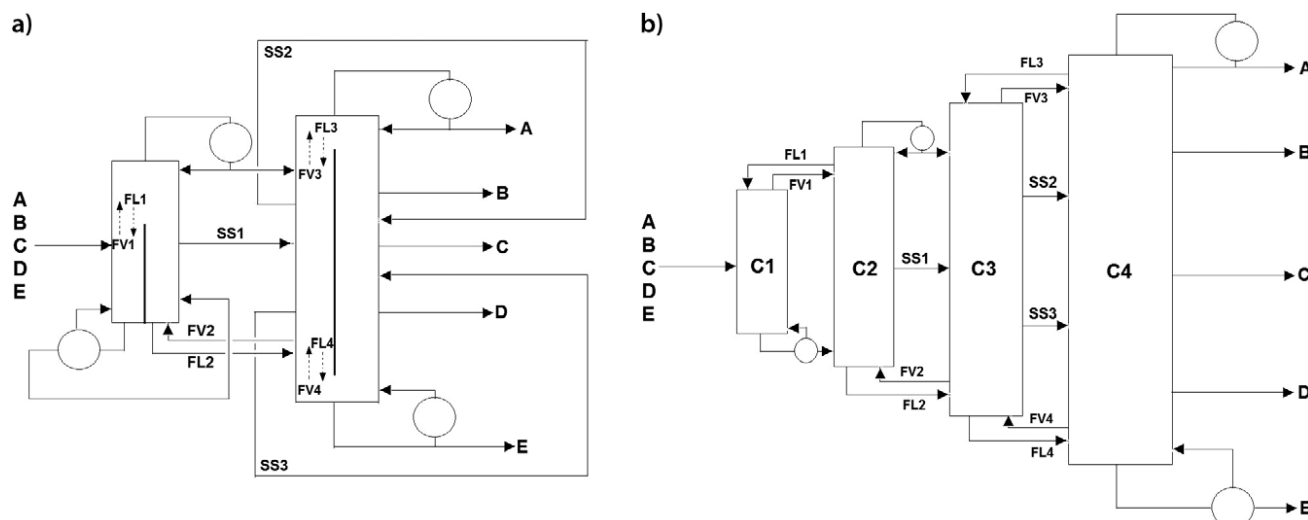


Figure 1. (a) Dividing-wall configuration for the separation of a five-component mixture, (b) thermodynamically equivalent configuration for simulation purposes.

ponents in a process with $N-1$ columns, on the other hand, the non-basic sequences are those which do not accomplish the separation in $N-1$ columns. The target is indeed to detect those basic alternatives that can be rearranged in intensified sequences, i.e., those which accomplish the separation task in less than $N-1$ columns.

The generation of logical relationships considering Boolean or binary variables can be included in a mathematical modeling, and that systematically includes all the sequences of the separation task that can be rearranged in $N-1$ distillation columns. The entire description of this methodology can be found in many works, e.g., in [28]. As this model formulation does not rely on any specific column configuration, it is considered here as the starting point for generating intensified sequences.

Once the basic sequences that can be rearranged are identified, the next step is to characterize the thermodynamically equivalent configurations. So, starting with any configuration among all the thermodynamically equivalent alternatives, the following steps allow generating the DWC alternatives.

- Two columns connected by just a single thermal couple can be rearranged in a CVP. (Fig. 2).

- Two columns connected by a thermal couple and a regular heat exchanger can also be rearranged in a DWC, but in this case the stream connecting both columns must be externally transferred to the correct side of the column. Fig. 2 b clarifies this point.
- Two columns connected by two thermal couples, without any connection between them, can be rearranged in a DWC.
- If two columns are connected by more than two streams, then one must differentiate two cases: a) The intermediate connections are liquid streams, and b) the intermediate connection is a thermal couple. In case a), the liquid streams are transferred directly to the correct part of the wall (Fig. 3 a). In the second case, it is possible allowing a bidirectional transfer flow through the wall (Fig. 3 b). However, in this case, there are difficulties in the operation of the column.
- The next step is to remove column sections. Errico et al. [29] reported that it is possible to remove some intermediate columns formed by a single section without excessive energy penalty and therefore reducing the number of actual columns (Figs. 4 a–c). Using that set of equations and enforcing that at least one column is formed by a single section easily permits to obtain those configurations.

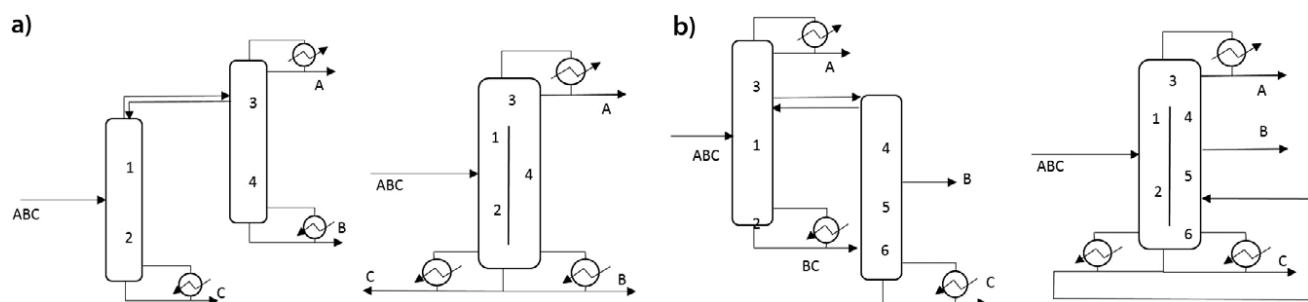


Figure 2. (a) Arrangement of an indirect distillation sequence connected by a single thermal couple in a DWC, (b) rearrangement in a single shell of a direct distillation sequence connected by a thermal couple and a regular heat exchanger.

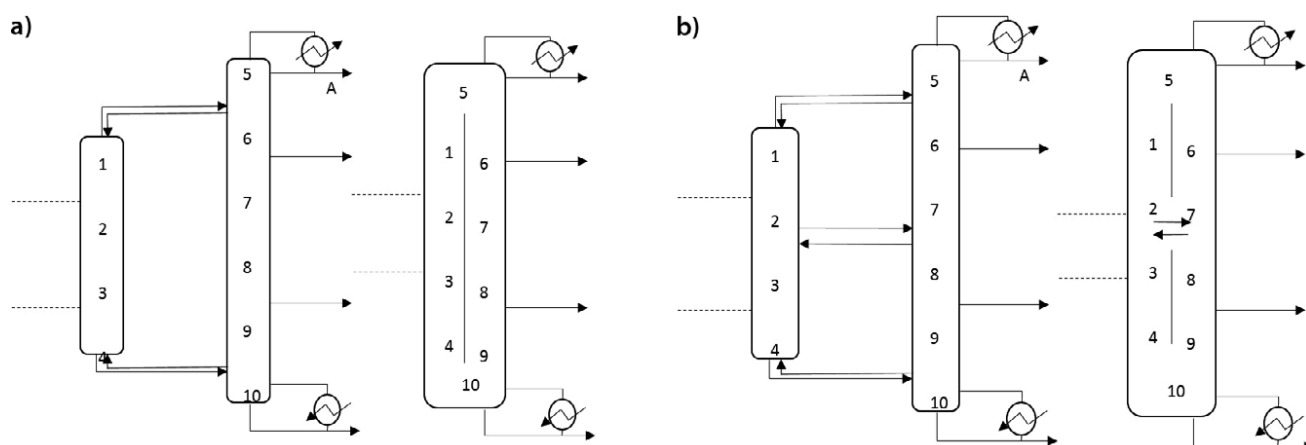


Figure 3. (a) Generation of a DWC by transfer of the liquid stream of two columns, (b) DWC with two vertical walls and liquid and vapor transfer in the intermediate zone.

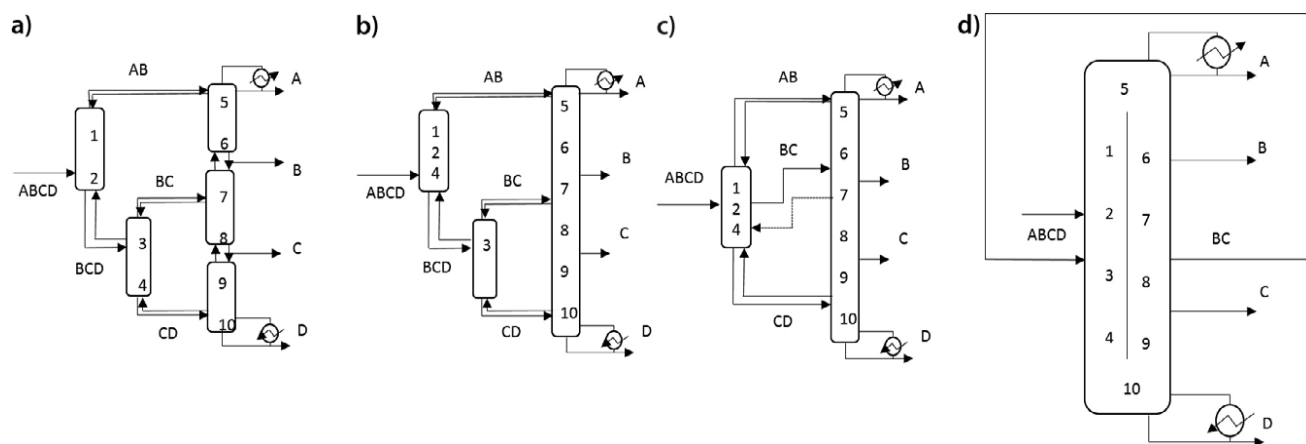


Figure 4. Procedure to remove a section column. (a) Sequence of separations, each column is a separation task, (b) rearrangement in three columns with a column formed by a single section, (c) sequence after removing section 3, (d) final arrangement in a single column with an internal wall and external liquid transfer.

3.2 Steady-State Simulation

Steady-state simulations of the system presented in Fig. 1 b were performed in Aspen Plus V8.4. Structural design parameters for each column were taken from the work of Caballero and Reyes-Labarta [26] and are presented in Tab. 2, where N_T ¹⁾ is the total number of stages, N_F is the stages where feed streams enter to the column, and N_{SS} are the stages from which side streams are withdrawn. Such parameters were obtained through short-cut methods.

The pressure is set as 1 bar for the top section of column C4, with a total pressure drop of 0.68 bar from top to bottom. To determine the pressure in the other columns, it was assumed that the pressure drop per stage in C4 is the ratio between total pressure drop and the number of stages. Then, the top and bottom pressure for C3 was estimated backwards, in terms of the pressure for the interlinking stages in C4. The same procedure

Table 2. Design characteristics of the columns.

	C1	C2	C3	C4
N_T	6	16	34	89
N_F	1, 3	4, 12, 17	1, 6, 17, 28, 35	11, 33, 55, 77
N_{SS}	–	8, 10	11, 22, 28	11, 22, 44, 66, 77

was followed to estimate top and bottom pressure for C1 and C2. Once the required purities were fixed through the Design Specification tool of Aspen Plus, using the reflux ratio, heat duty, and side stream flow rates to reach the desired purities, a sensitivity analysis was performed, taking as degrees of freedom the interlinking streams $FL1$, $FV2$, $FL3$, and $FV4$.

Due to the high convergence time required to simultaneous analyzing the four streams, a systematic approach was used. First, the flow rates of $FL1$, $FV2$, and $FL3$ were fixed, and a sensitivity analysis was performed over $FV4$, using the Sensitivity tool of Aspen Plus. Once the results were obtained, the value of

1) List of symbols at the end of the paper.

FL3 was manually modified, and the sensitivity analysis was performed for FV4. FL1 and FV2 were modified in a similar way to FL3.

Fig. 5 presents a flow chart for the optimization procedure. The side streams molar flow rate was fixed as $SS1 = 60 \text{ kmol h}^{-1}$, $SS2 = 40 \text{ kmol h}^{-1}$, $SS3 = 60 \text{ kmol h}^{-1}$, as reported by Caballero and Reyes-Labarta [26]. From the sensitivity analysis, seven points with different heat duties were selected to be analyzed in a dynamic state. It is important to recall that all the seven selected points had the same configuration as presented in Tab. 2, and they differed only in the molar interlinking flow rates.

3.3 Open-Loop Dynamic Analysis

To compare the dynamic performance of the cases already designed, a control analysis was performed by means of the singular value decomposition (SVD) in an open-loop control test. This technique was carried out to obtain a comparative framework on the control properties of all schemes. The SVD technique is a quite useful tool in linear system theory. Lau et al. [30] and Bequette [31] applied the SVD technique on distillation models. Besides, this technique was also employed for studying complex separation schemes based on distillation [32–34]. Through several studies on separation schemes, SVD demonstrated that under certain conditions, multivariable model-based techniques result in controllers that can be decomposed into the SVD structure [33]. The SVD technique can

be regarded both as a true multivariable controller and as a control structure for decentralized design [34].

An appealing feature of the SVD controller is that it is only slightly more complicated than a decentralized controller, but the achievable performance is not limited in the same way. Sagfors and Walle [35] showed that for distillation systems SVD is a feasible control structure, even if a quantitative model is lacking. On the other hand, Hovd et al. [34] claim that even if a quite good model is available and some model-based technique is applied, it is very possible to end up with a controller which is indeed very close to the SVD controller anyway. Moreover, SVD plays a key role when the control properties of a process in real industry are studied [36]. SVD determines the rank and the condition of a matrix and is quite useful to geometrically chart the strengths and weaknesses of a set of equations [36]. The general methodology to perform the SVD analysis for our case of study is described below.

Initially, all DWC schemes were exported from steady state to dynamic state for its analysis in Aspen Dynamic. In such platform, all the selected cases were subjected to a disturbance in the associated manipulated variable: reflux ratio of column for nC6, reboiler heat duty for nC10, and side stream flow rates for nC7, nC8, and nC9, all the variables corresponding to column C4. The magnitude of that perturbation was set as a 0.5 % positive change in the values of those manipulated variables on its nominal state. Each manipulated variable was chosen according to each product stream, i.e., when a component was purified in the top of a distillation column, the manipulated variable was the reflux ratio; however, if the purified component remained in the distillation column as a bottom product, the manipulated variable was the reboiler heat duty, and so on.

When all responses were obtained, the matrices of transfer functions (G) were collected to perform the SVD calculation. The calculation of SVD can be summarized as follows:

$$\mathbf{G} = \mathbf{V}\Sigma\mathbf{W}^H \quad (1)$$

where $\Sigma = \text{diag}(\sigma_1, \sigma_2, \dots, \sigma_n)$, σ_1 is the singular value of $\mathbf{G} = \lambda^2(\mathbf{G}\mathbf{G}^H)$, $\mathbf{V} = (v_1, v_2, \dots, v_n)$ is the matrix of left singular vectors, and $\mathbf{W} = (w_1, w_2, \dots, w_n)$ is the matrix of right singular vectors. From the decomposition, the two parameters of interest are the minimum singular value σ^* and the ratio of the maximum to minimum singular values, named the condition number, which is calculated as follows:

$$\gamma^* = \sigma^*/\sigma_1 \quad (2)$$

The engaging aspect of the SVD study regarding to the process control is that, when applied to a matrix which describes the steady-state characteristics of a multivariable process, the singular values have a strong physical interpretation. Very small singular values could indicate that, despite of a good condition number, the system is not quite sensitive enough to control. On the other hand,

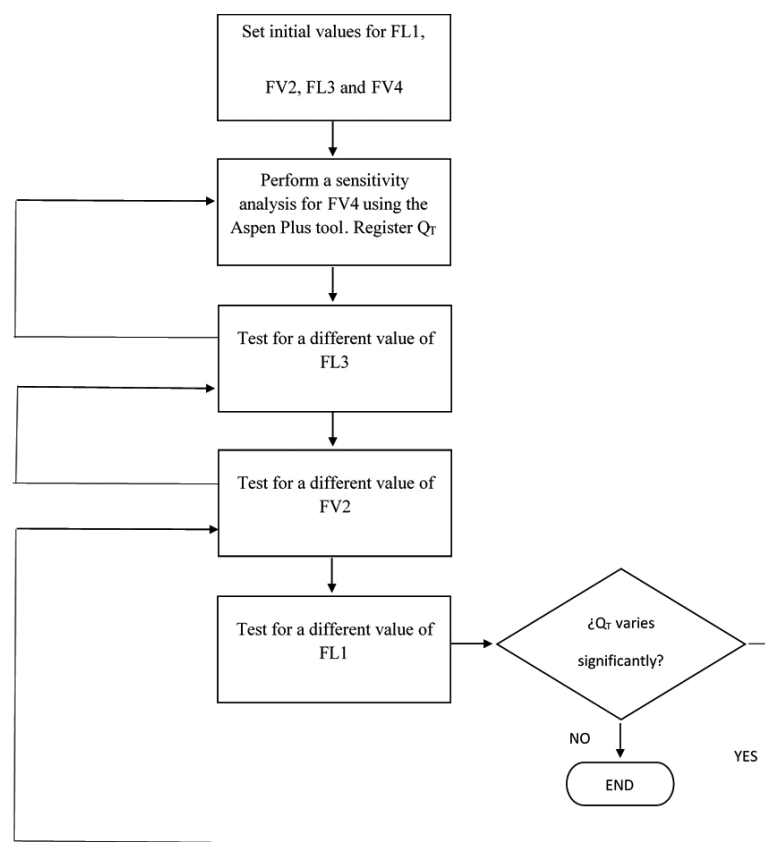


Figure 5. Flow chart for the optimization procedure.

large singular values point to a practical control problem [35]. Furthermore, the condition number could be interpreted as the sensitivity of the system under uncertainties and modeling errors. However, the condition number only provides a qualitative assessment of the theoretical control properties of the schemes under analysis [34].

In physical terms, the condition number represents the ratio of the maximum and minimum open-loop, decoupling gains of the system. A large condition number means that the relative sensitivity of the system in one multivariable direction is very weak [34]. SVD analyses do not predict or solve all the control problems which may be found in the industrial operability, however, are relatively easy to understand and identify basic control difficulties. The SVD technique was used by several authors to study the dynamic properties of complex designs [30,39]. In this work, once the matrices of transfer functions were obtained, the singular value decomposition was identified through a code in MATLAB.

3.4 Closed-Loop Analysis Dynamic

As a second control analysis, the closed-loop test was performed in two studies: 1) a step change was induced in the set point and 2) a 3% change in the total feed stream was implemented as feed disturbance. Similar as the open-loop test, the closed-loop analysis was performed in Aspen Dynamics. It must be highlighted that for exporting from Aspen Plus to Aspen Dynamics it is necessary to set the rigorous hydraulics and column pressure drop on. This is the reason why, once the design is exported to Aspen Dynamics, the pressure and control level are set as default. Besides it is reported that both, level or pressure, do not have the influence that either composition or temperature may have [40].

Notice that the compound that was monitored was octane, since this dynamic response was considered as representative for the closed-loop test because of the amount of octane in the feed stream. Moreover, a set of three schemes was considered: CASE1, CASE4, and CASE7, selected as representative cases in terms of the regions for total energy requirements. For the closed-loop control policy, the analysis was based on proportional-integral (PI) controllers, because of its wide use in industrial practice. When a controller is applied, a main issue is to tuning the controller. Since PI controllers were considered, the proportional gain (K_c) and the reset times were tuned up for each scheme studied here, having as performance criteria the integral of absolute error (IAE) criterion [41].

For the tuning process, an initial value of proportional gain was set, and a range of integral reset time was tested with this fixed value until a local optimum in the IAE value was obtained. This methodology was repeated with other proportional gain values until a global minimum was found for the IAE.

In order to select the control outputs and its respective manipulated variables, the LV control structure was used, which takes the reflux flow rate L and the vapor boil up rate V as the manipulated variables [42]. This type of control loop was applied with satisfying results for the study of thermally coupled schemes [43,44].

4 Results

4.1 Steady-State Simulation

Tab. 3 presents the selected solutions from the sensitivity analysis, where RR is the reflux ratio and Q_T is the total heat duty, given by the sum of heat duties for columns C1 and C4. The two first cases (case 1 and case 2) are solutions with the lowest energy requirements. Cases 3, 4, and 5 have mid values of heat duty, while the last two cases (case 6 and case 7) are selected from a region with high energy requirements.

While the reflux ratio for column C2 ranges from 2.2 to 3.5, that for column C4 varies between 18.34 and 171.45, with continuous increasing from case to case. It is important to mention that, for cases 1, 2, and 3, the contribution of C4 to the total heat duty is around 70%, while for cases 6 and 7 that column contributes with 93% of the total heat duty. This occurs because the heat duty for column C1 remains almost constant when modifying the interlinking flow rates, while the heat duty of column C4 is quite sensitive to such changes. To better understand the effect of the interlinking flow rates, Fig. 6 gives a comparison for the liquid and vapor flow rates for all the studied cases.

It can be seen that the cases with the lowest heat duty exhibit the lowest values for the liquid interlinking streams. This is particularly noticeable for $FL2$ and $FL4$. On the other hand, the cases with the highest duty also have the highest values for the liquid interlinking flow rates. A similar trend is observed for $FV2$. Nevertheless, the opposite occurs for $FV3$, where the cases with lowest duty showed low values for that flow rate. Thus, in terms of heat duty, relatively low flow rates must be preferred, but enough to satisfy mass balances, except for the vapor stream feeding the upper region of column C4, where a high flow rate is preferred. This stream contains mainly the light

Table 3. Selected cases from the sensitivity analysis.

Case	$FL1$ [kmol h ⁻¹]	$FV2$ [kmol h ⁻¹]	$FL3$ [kmol h ⁻¹]	$FV4$ [kmol h ⁻¹]	RR_{C2}	RR_{C4}	Q_T [kW]
Case 1	80	40	36	110	2.29	18.34	5647.44
Case 2	80	45	36	112	2.36	19.35	5857.47
Case 3	85	70	42	130	2.81	35.64	8807.69
Case 4	85	80	40	130	2.97	61.12	13 047.76
Case 5	85	65	38	110	2.74	80.68	16 082.03
Case 6	85	95	52	130	3.35	150.55	27 709.02
Case 7	85	95	40	110	3.43	171.45	31 057.02

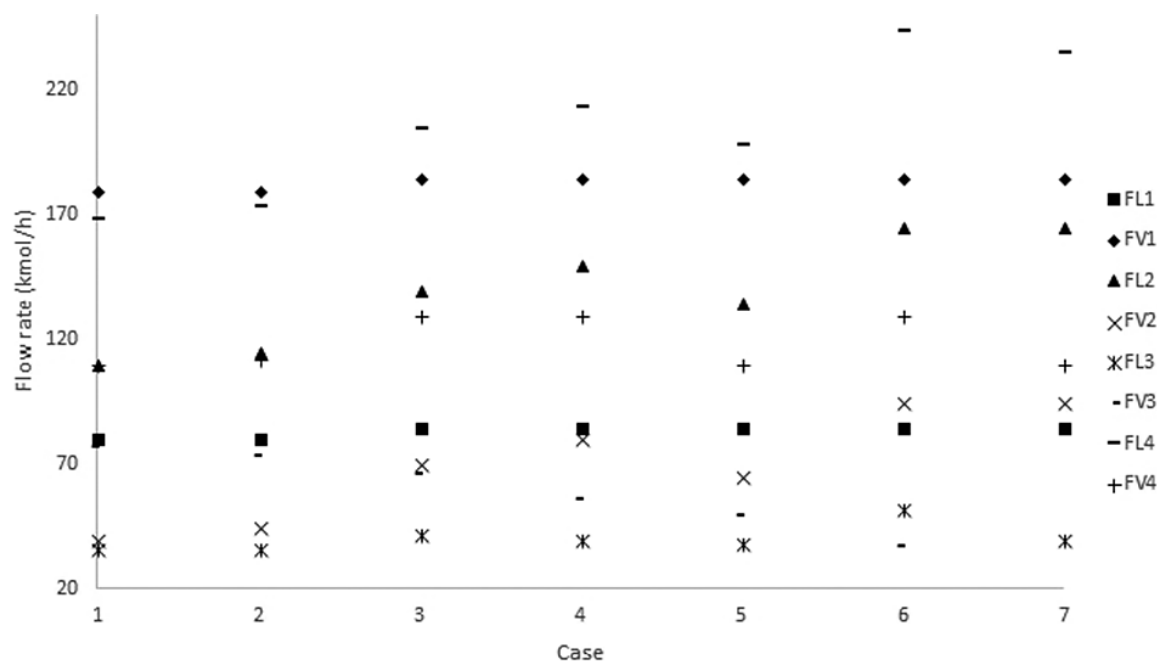


Figure 6. Interlinking flow rates for the studied cases.

components, i.e., *n*-hexane and *n*-heptane, which are in a relatively low concentration in the feed stream.

Tab.4 shows the diameters for each column, computed through the Tray Sizing tool of Aspen Plus. The diameter for columns C1 and C3 remains almost constant, while that for columns C2 and C4 change from case to case. Nevertheless, the diameter for column C2 ranges between 1.4 and 1.7 m, which is only a small variation, while the diameter for column C4 varies considerably, from 2 to almost 7 m. The results in Tabs. 3 and 4 indicate a high sensitivity of the last column to changes on the interlinking flow rates.

Table 4. Computed diameters (m).

Case	C1	C2	C3	C4
Case 1	1.40	1.45	1.12	2.03
Case 2	1.40	1.46	1.13	2.09
Case 3	1.42	1.57	1.21	2.83
Case 4	1.42	1.60	1.21	3.72
Case 5	1.42	1.55	1.11	4.27
Case 6	1.41	1.66	1.21	6.12
Case 7	1.41	1.67	1.11	6.60

4.2 Open-Loop Dynamic Simulation

In this section, results for the open-loop analysis are presented and discussed. Fig.7 presents an example of the dynamic responses obtained. It corresponds to the responses when perturbing the reflux ratio of column C4 for case2. All the

responses for the presented case were stable before 10 h, showing no oscillations.

Tab.5 presents the matrix of transfer functions for case2 in order to exemplify the kind of transfer functions obtained in the study. The rows are related with the variables to which perturbations are applied, while the columns are related to the mole composition of the component *j* in the corresponding product stream of the column C4. It can be seen that even for the complex system under study all the responses were adjusted as first order or first order in competence.

Fig. 8 displays the results for the minimum singular value for $0 \leq \omega \leq 100 \text{ rad h}^{-1}$, which is a range of realistic physical sense [36]. It is important to recall that the scale for both plots is logarithmic and that the systems with high values of σ_* are preferred.

If the region below 0.01 rad s^{-1} of Fig. 8 is analyzed, it can be seen that case 1 shows the highest minimum singular value, followed by cases 4 and 7. Case 2 exhibits the worst values for σ_* in that range. On the other hand, for frequencies higher than 1 rad s^{-1} , clear trends can be observed, where case 1 remains as the best one in terms of σ_* . The other cases can be ordered as follows, from higher to lower values of σ_* : case 2, case 3, case 5, case 4, case 6, case 7. It can be seen that for $\omega \geq 1 \text{ rad s}^{-1}$, there is a trend in which the cases with the lowest heat duty showed the best values for σ_* , while the cases with the highest energy requirements displayed the worst values.

Fig. 9 presents the condition number for the range of frequencies of interest. For frequencies lower than 0.01 rad s^{-1} , case 1 showed the lowest values for the condition number, which is a desired performance. Case 2 presented the highest values of the condition number for frequencies below 0.1 rad s^{-1} , then a variation in trend was observed. For frequencies higher than 1 rad s^{-1} , cases 1 and 2 showed low values of γ^* , while the condition numbers increased gradually for case 5,

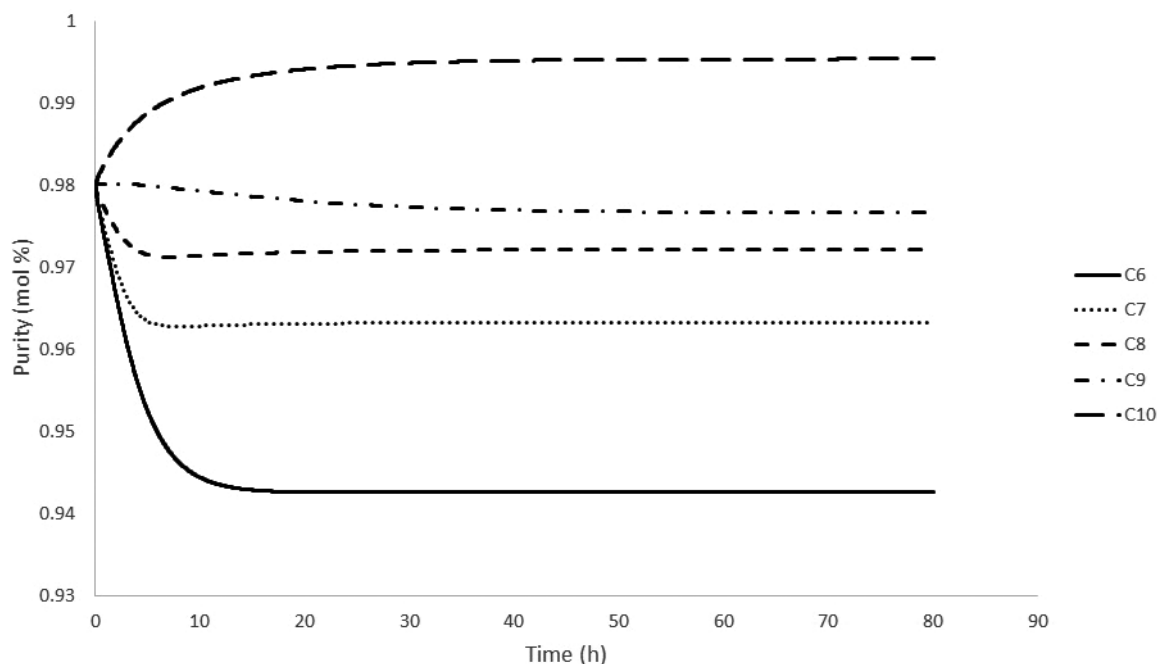


Figure 7. Dynamic responses for the perturbation in reflux ratio, case 2.

Table 5. Matrix of transfer functions for case 2.

	x_{nC6}	x_{nC7}	x_{nC8}	x_{nC9}	x_{nC10}
RR_{C4}	$\frac{-14.9524}{1 + 3.6272\tau s}$	$\frac{0.4}{1 + 3.34s} + \frac{0.2284}{1 + 8.25s}$	$\frac{-1.8196}{1 + 5.22\tau s}$	$\frac{-0.9812}{1 + 4.62\tau s}$	$\frac{7.9908}{1 + 2.90\tau s}$
F_B	$\frac{1.597995}{1 + 0.70397\tau s}$	$\frac{5.4754}{1 + 1.14\tau s}$	$\frac{0.12}{1 + 3.239s} + \frac{0.04}{1 + 8.24s}$	$\frac{-0.6824}{1 + 2.26\tau s}$	$\frac{7.8}{1 + 2.929s} + \frac{-8.521}{1 + 7.53s}$
F_C	$\frac{-2.2}{1 + 1.501s} + \frac{-0.926}{1 + 8.231s}$	$\frac{1.665}{1 + 0.306s} + \frac{-0.038}{1 + 0.431s}$	$\frac{-14.9296}{1 + 3.17\tau s}$	$\frac{-0.5284}{1 + 1.5\tau s}$	$\frac{0.9216}{1 + 0.06\tau s}$
F_D	$\frac{-0.8948}{1 + 1.2\tau s}$	$\frac{-7.2036}{1 + 3.88\tau s}$	$\frac{-14.9524}{1 + 3.6272\tau s}$	$\frac{0.0412}{1 + 0.06\tau s}$	$\frac{-2.6732}{1 + 5.05\tau s}$
Q_{C4}	$\frac{6.1752}{1 + 7.29\tau s}$	$\frac{-26.4876}{1 + 3.4\tau s}$	$\frac{-43.7936}{1 + 3.06\tau s}$	$\frac{-49.09}{1 + 7.625\tau s}$	$\frac{-13.468}{1 + 3.07\tau s}$

case 4, case 6, case 3, and case 7. For the condition number, the two cases with lowest heat duty presented the best values, while the other cases did not show a given trend. Particularly, case 3 exhibited important variations in the values of γ^* for different ranges of frequency.

To obtain a more reliable parameter for comparing the performance of the condition number, the area below each curve was determined, as reported by Cabrera-Ruiz et al. [36]. In this work, each curve was adjusted to a proper function, and the defined integral was computed. Tab. 6 summarizes the computed values for the areas below the condition number curves.

The case with the lowest heat duty, i.e., case 1, had the lowest area below its condition number curve, followed by case 2. The other cases can be ordered from lower to higher area as follows: case 5, case 4, case 6, case 3, case 7. In general terms, the cases with lowest duties showed the best control properties. Those cases had the lowest values for $FV2$ and $FL2$, which are the

vapor stream going from the lower region of the second DWC to the first one and the liquid stream going from the lower region of the first DWC to the second one, respectively.

Moreover, the cases with the best control properties had relatively high flow rates for $FV3$, the vapor stream feeding the upper zone of the column $C4$, but relatively low values for the liquid and vapor streams leaving and feeding, respectively, the lowest zone of the same column. This implies that the cases with lowest heat duty, case 1 and case 2, had lower internal flow rates, implying better control properties. The other cases, which presented relatively bad control properties, had higher internal flow rates. The two first cases, which provided the best dynamic performance, also had the smallest diameters for column $C4$.

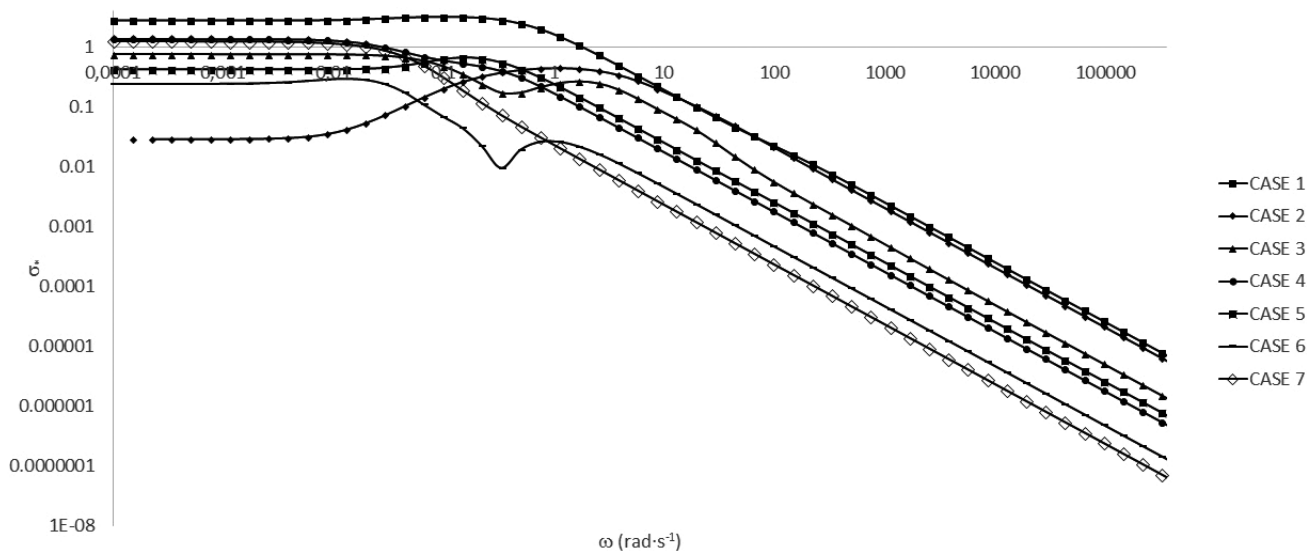


Figure 8. Minimum singular value.

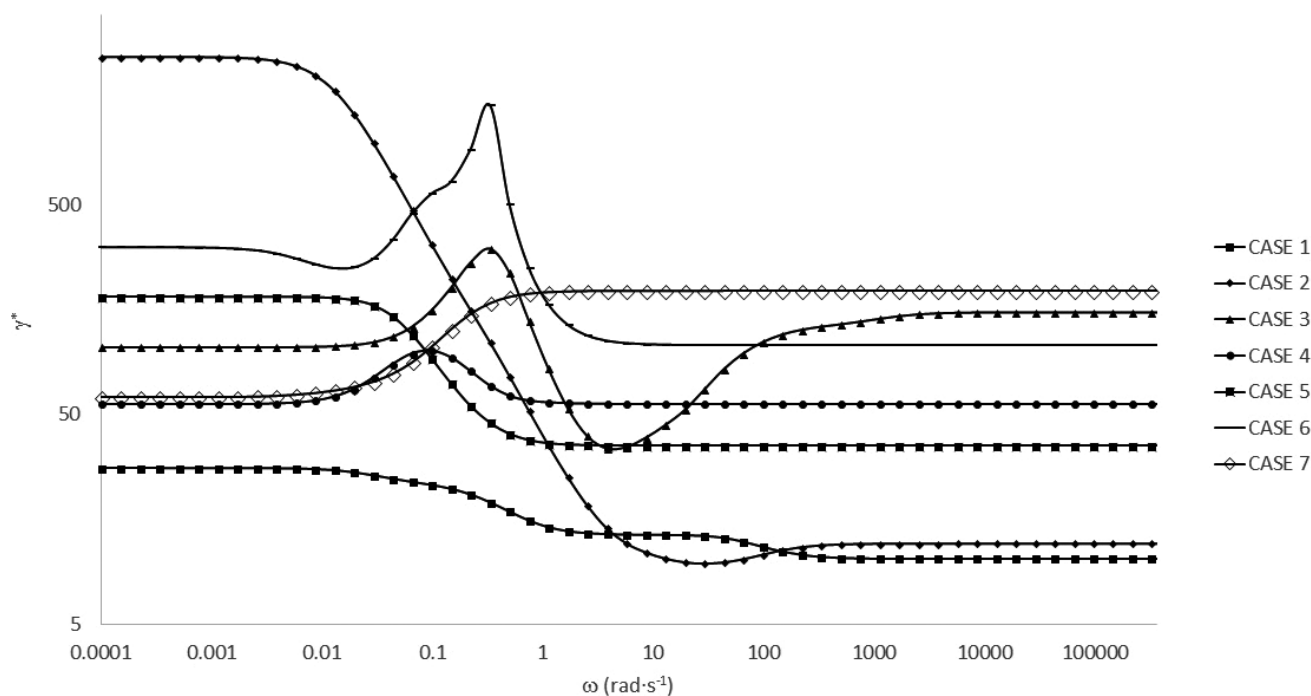


Figure 9. Condition number.

4.3 Closed-Loop Dynamic Simulation

Regarding the closed-loop control test, as mentioned before, the closed-loop simulations were performed initially introducing a step change in the set point for the product composition of octane under a single-input/single-output feedback control for cases 1, 4, and 7.

The results from the individual servo test applied to the reference case and the thermally coupled designs are illustrated in Fig. 10. Notice that case 1 showed the lowest settling times, near

0.08 h, in comparison with case 4 and 7 with 0.73 and 2.91 h, respectively. Those settling times were further proved with the IAE values of Tab. 7, in other words, Case 1 exhibited the lowest IAE values in comparison with both, case 4 and 7. Considering the general design parameters of all cases (Tab. 2), the trend is clear. For this case of study, case 1 had the lowest IAE, and also it is designed with the lowest energy requirements. Otherwise, case 7 showed the highest IAE values and also the highest energy requirements. Under this scenario, this kind of separation alternatives seems to be able of working with low

Table 6. Areas below the condition number curves.

Case	Area
Case 1	98 973.38
Case 2	112 526.00
Case 3	1 219 037.37
Case 4	517 720.90
Case 5	288 409.04
Case 6	1 051 484.21
Case 7	1 774 771.83

energy requirements without apparent penalties on its dynamic behavior. The K_c and τ values for the tuning process are described in Tab. 7.

Regarding the second closed-loop analysis and observing Fig. 11, it can be concluded that the test followed the same trend than that observed in the set point change. Notice that after disturbance in the total molar flow, case 1 reached the nominal set point in a shorter time than case 4 and 7. This behavior is also corroborated with the IAE values of Tab. 7.

From the previous evidence, it is possible to conclude for the close-loop analysis that this kind of schemes are able to handle disturbances, either as a set point change or as a total mole flow change. Moreover, this control capabilities do not seem to have a control cost since the case who showed the best dynamic performance is indeed the scheme with the lowest energy requirement, the lowest reflux ratios, and relatively the lowest diameters. Therefore, these results indicate that the industrial implementation of this complex distillation column is possible because it presents energy savings simultaneously with a good dynamic performance.

In the particular case of industrial implementation of the control structures, a practical idea would be the one proposed

Table 7. K_c , τ_{ii} and IAE values for the tuning process.

Octane			
	K_c	τ_i [min]	IAE
<i>Set point change</i>			
Case 1	250	1	3.17×10^{-4}
Case 4	250	5	1.29×10^{-3}
Case 7	250	5	4.24×10^{-3}
<i>Feed disturbance</i>			
Case 1	250	1	1.82×10^{-5}
Case 4	250	5	3.20×10^{-5}
Case 7	250	5	2.49×10^{-4}

by Kaibel and Stroezel [45] in their patent. They suggest measurements of concentration at specific points in each section separated by a partition wall by direct or indirect measuring techniques, to create a necessary control interface. Another idea is proposed by Zavala-Guzmán et al. [46] who proposed a systematic technique to tune PI controllers for a class of complex columns with periodic discrete measurements. Provided classical parameters of the process dynamics and the sampling delay time of measurements, this technique determines effective gains for every controller of complex arrangement in a straightforward and simultaneous way. If a certain adjustment is needed, it is done through a tuning parameter associated with a desired convergence rate, meaning a significant reduction in trial-and-error tuning. This technique is the discrete counterpart of the one applied for a complex column with continuous measurement of the composition with good results, and it is expected to be applicable for any multiple-input multiple-output (MIMO) control system.

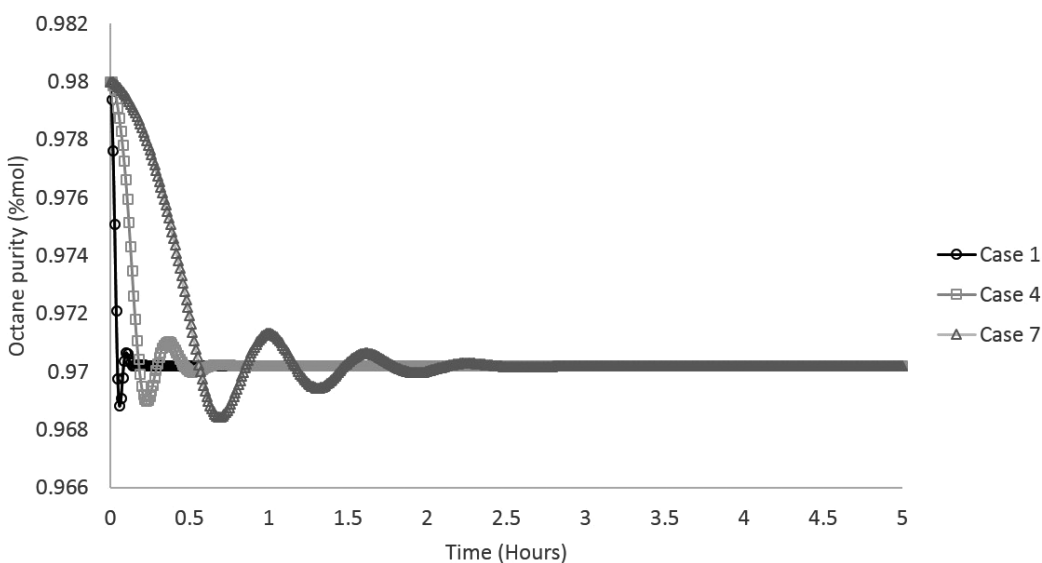


Figure 10. Dynamic behavior of case 1, 4, and 7 under a set point change.

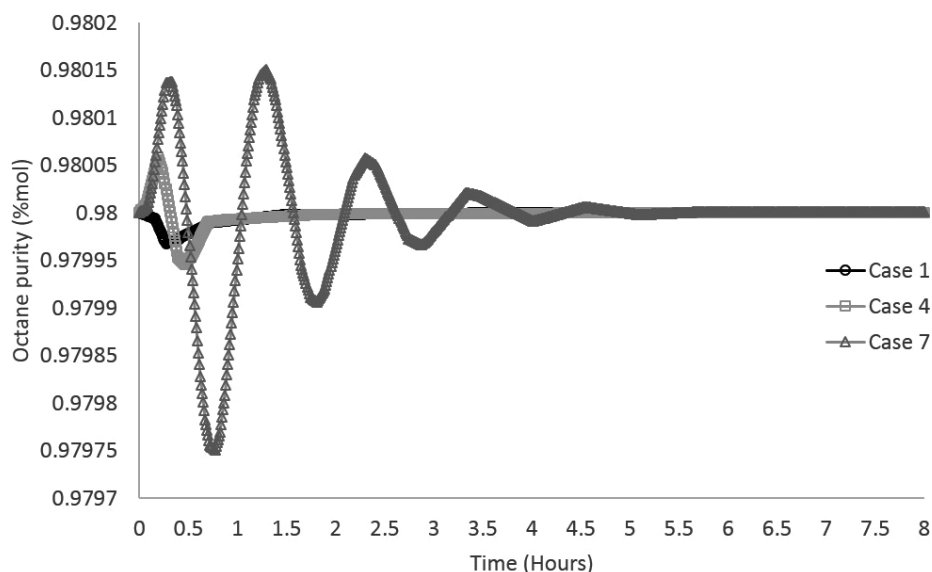


Figure 11. Dynamic behavior of case 1, 4, and 7 under a disturbance in the feed flow rate.

An important aspect to highlight is the effect of the variation of the design specifications of the distillation column on the control properties of the column. As indicated by Gomez-Castro et al. [33] the variation of the design specifications of a complex distillation column, particularly the modification of the values of the interconnection flows, affects the control properties and energy consumption of the complex distillation arrangement. Therefore, the results obtained in this work are consistent with those reported in the literature about the fact that the modification of the values of the interconnection flow rates modifies the control properties and energy consumption. This has also been reported for complex reactive and extractive distillation sequences [32].

5 Conclusions

An open-loop analysis of a complex configuration of multi-component distillation was presented. Dynamic properties, i.e., minimum singular value and condition number were obtained for the studied column under different operation conditions, and a closed-loop analysis was performed. In terms of steady-state design, it was found that the vapor interlinking flow rate between both DWCs had great influence on the total heat duty. Moreover, the two designs with lower values of heat duty, namely case 1 and 2, which also showed the lowest values of FV2 among all the selected cases, exhibited better dynamic properties. On the other hand, the designs with high energy requirements presented bad dynamic properties.

Acknowledgment

The authors acknowledge the support of the Universidad de Guanajuato for the development of this work.

The authors have declared no conflict of interest.

Appendix A Transfer Function Matrices

Transfer function matrices are generated by implementing step changes in the manipulated variables of the design of the distillation sequence and registering the dynamic responses of the five products. The product streams' purity is one of the most common variables analyzed for initial controls studies on distillation columns [32–47]; then, the only output variable studied for each product stream was the molar fraction. For instance, if the molar fraction of component i in the distillate flow was defined as output variable, the selected control variable directly related to the distillate purity is the reflux ratio. In the same way, for the molar fraction of component j in the bottom flow, the selected control variable directly related to the residue purity is the reboiler duty. Finally, regarding the molar fraction of component k in the side stream, the flow rate was selected as control variable directly related to its purity.

The next matrix (A1) summarizes the input and output variables and disturbances as well for the case study.

$$\begin{bmatrix} nC6 \\ nC7 \\ nC8 \\ nC9 \\ nC10 \end{bmatrix} = \begin{bmatrix} g_{1,1}(k_{1,1}\tau_{1,1}) & g_{1,2}(k_{1,2}\tau_{1,2}) & g_{1,3}(k_{1,3}\tau_{1,3}) & g_{1,4}(k_{1,4}\tau_{1,4}) & g_{1,5}(k_{1,5}\tau_{1,5}) \\ g_{2,1}(k_{2,1}\tau_{2,1}) & g_{2,2}(k_{2,2}\tau_{2,2}) & g_{2,3}(k_{2,3}\tau_{2,3}) & g_{2,4}(k_{2,4}\tau_{2,4}) & g_{2,5}(k_{2,5}\tau_{2,5}) \\ g_{3,1}(k_{3,1}\tau_{3,1}) & g_{3,2}(k_{3,2}\tau_{3,2}) & g_{3,3}(k_{3,3}\tau_{3,3}) & g_{3,4}(k_{3,4}\tau_{3,4}) & g_{3,5}(k_{3,5}\tau_{3,5}) \\ g_{4,1}(k_{4,1}\tau_{4,1}) & g_{4,2}(k_{4,2}\tau_{4,2}) & g_{4,3}(k_{4,3}\tau_{4,3}) & g_{4,4}(k_{4,4}\tau_{4,4}) & g_{4,5}(k_{4,5}\tau_{4,5}) \\ g_{5,1}(k_{5,1}\tau_{5,1}) & g_{5,2}(k_{5,2}\tau_{5,2}) & g_{5,3}(k_{5,3}\tau_{5,3}) & g_{5,4}(k_{5,4}\tau_{5,4}) & g_{5,5}(k_{5,5}\tau_{5,5}) \end{bmatrix} \begin{bmatrix} RR_{C4} \\ F_B \\ F_C \\ F_D \\ Q_{C4} \end{bmatrix} \quad (A1)$$

where g represents the transfer function, $\tau_{i,j}$ is the dominant time constant for each disturbance realized, k is the gain for each disturbance realized, RR means the reflux ratio, F the flow rate, and Q represents the reboiler heat duty.

After the design was obtained, open-loop dynamic simulations were carried out in Aspen Dynamics in order to obtain the transfer function matrix (A1). For the case of study considered here, the transfer function matrix was generated by using step changes (1% of nominal value) in each manipulated variable and recording the dynamic behavior of the five product compositions. It can be observed that dynamic responses can be adjusted to first order or parallel processes.

Symbols used

FL_i	[kmol h ⁻¹]	liquid interlinking flow rate
FV_i	[kmol h ⁻¹]	vapor interlinking flow rate
F_j	[kmol h ⁻¹]	mole flow rate of product j
G	[-]	matrix of transfer functions
N_F	[-]	location of feed stages
N_{SS}	[-]	location of side streams
N_T	[-]	total number of stages
Q_T	[kW]	total heat duty
SS_i	[kmol h ⁻¹]	side stream flow rate
V	[-]	matrix of left singular vectors
W	[-]	matrix of right singular vectors
x_{Fj}	[-]	mole composition of component j in the feed stream
x_j	[-]	mole composition of component j in the corresponding product stream

Greek letters

$\alpha_{j,HK}$	[-]	relative volatility of component j and heavy component
γ^*	[-]	condition number
Σ	[-]	matrix of singular values
σ^*	[-]	minimum singular value
σ^*	[-]	minimum singular value
ω	[rad s ⁻¹]	frequency

Abbreviations

DWC	dividing-wall column
IAE	integral of absolute error
SVD	singular value decomposition

References

- [1] M. R. Hernández, J. A. Chinea-Herranz, *J. Process Control* **2012**, 22 (9), 1582–1592. DOI: <https://doi.org/10.1016/j.jprocont.2012.06.015>
- [2] J. Fang, H. Zhao, J. Qi, C. Li, J. Qi, Guo, *Chin. J. Chem. Eng.* **2015**, 23 (6), 934–940. DOI: <https://doi.org/10.1016/j.ces.2017.12.011>
- [3] S. T. Holland, R. Abbas, D. Hildebrandt, D. Glasser, *Ind. Eng. Chem. Res.* **2010**, 49 (1), 327–349. DOI: <https://doi.org/10.1021/ie801752r>
- [4] P. Kumari, R. Jagtap, N. Kaistha, *Ind. Eng. Chem. Res.* **2014**, 53 (42), 16436–16452. DOI: <https://doi.org/10.1021/ie5021409>
- [5] M. A. Schultz, D. G. Stewart, J. M. Harris, S. P. Rosenblum, M. S. Shakur, D. E. O'Brien, *Chem. Eng. Prog.* **2002**, 98 (5), 64–71.
- [6] I. Dejanovic, L. J. Matijasevic, Z. Olujic, *Chem. Eng. Process.* **2010**, 49 (6), 559–580. DOI: <https://doi.org/10.1016/j.ccep.2010.04.001>
- [7] B. G. Rong, *Chem. Eng. Res. Des.* **2011**, 89 (8), 1281–1294. DOI: <https://doi.org/10.1016/j.cherd.2011.03.014>
- [8] A. A. Kiss, D. J.-P. C. Suszwalak, *Sep. Purif. Technol.* **2012**, 86, 70–78. DOI: <https://doi.org/10.1016/j.seppur.2011.10.022>
- [9] Q.-K. Le, I. J. Halvorsen, O. Pajalic, S. Skogestad, *Chem. Eng. Res. Des.* **2015**, 99, 111–119. DOI: <https://doi.org/10.1016/j.cherd.2015.03.022>
- [10] C. Bravo-Bravo, J. G. Segovia-Hernández, C. Gutiérrez-Antonio, A. L. Durán, A. Bonilla-Petriciolet, A. Briones-Ramírez, *Ind. Eng. Chem. Res.* **2010**, 49 (8), 3672–3688. DOI: <https://doi.org/10.1021/ie9006936>
- [11] F. I. Gómez-Castro, V. Rico-Ramírez, J. G. Segovia-Hernández, S. Hernández-Castro, G. González-Alatorre, M. M. El-Halwagi, *Ind. Eng. Chem. Res.* **2012**, 51 (36), 11717–11730. DOI: <https://doi.org/10.1021/ie201397a>
- [12] J. A. Weinfeld, S. A. Owens, R. B. Eldridge, *Chem. Eng. Process.* **2018**, 123, 20–33. DOI: <https://doi.org/10.1016/j.ccep.2017.10.019>
- [13] A. A. Kiss, R. M. Ignat, S. J. Flores-Landaeta, A. B. de Haan, *Chem. Eng. Process.* **2013**, 67, 39–48. DOI: <https://doi.org/10.1016/j.ccep.2012.06.010>
- [14] A. C. Christiansen, S. Skogestad, K. Lien, in *Proc. of the 6th Distillation and Absorption* (Ed: R. Dalton), IChemE, UK **1997**, 745–756.
- [15] J. L. Blancarte-Palacios, M. N. Bautista-Valdés, S. Hernández, V. Rico-Ramírez, A. Jiménez, *Ind. Eng. Chem. Res.* **2003**, 42 (21), 5157–5164. DOI: <https://doi.org/10.1021/ie030297k>
- [16] X. Ge, B. Liu, X. Yuan, Y. Luo, K. K. Yu, *Chin. J. Chem. Eng.* **2017**, 25 (8), 1069–1078. DOI: <https://doi.org/10.1016/j.cjche.2017.03.018>
- [17] Y. Cho, B. Kim, D. Kim, M. Han, M. Lee, *J. Process Contr.* **2009**, 19 (6), 932–941. DOI: <https://doi.org/10.1016/j.jprocont.2008.12.003>

- [18] M. Rodríguez-Hernández, J. A. Chinea-Herranz, *J. Process Control* **2012**, *22* (9), 1582–1592. DOI: <https://doi.org/10.1016/j.jprocont.2012.06.015>
- [19] T. Egger, G. Fieg, *Chem. Eng. Sci.* **2018**, *179*, 284–295. DOI: <https://doi.org/10.1016/j.ces.2017.12.011>
- [20] G. Kaibel, *Chem. Eng. Technol.* **1987**, *10* (1), 92–98. DOI: <https://doi.org/10.1002/ceat.270100112>
- [21] D. Matla-González, G. Urrea-García, J. Alvarez-Ramirez, E. Bolaños-Reynoso, G. Luna-Solano, *Asia-Pac. J. Chem. Eng.* **2013**, *8* (6), 880–894. DOI: <https://doi.org/10.1002/apj.1733>
- [22] H. Ling, W. L. Luyben, *Ind. Eng. Chem. Res.* **2010**, *49* (1), 189–203. DOI: <https://doi.org/10.1021/ie900125w>
- [23] R. C. Van Diggelen, A. A. Kiss, A. W. Heemink, *Ind. Eng. Chem. Res.* **2010**, *49* (1), 288–307. DOI: <https://doi.org/10.1021/ie9010673>
- [24] J. C. Cardenas, S. Hernández, I. R. Gudiño-Mares, F. Esparza-Hernández, C. Y. Irianda-Araujo, L. M. Domínguez-Lira, *Ind. Eng. Chem. Res.* **2005**, *44* (2), 391–399. DOI: <https://doi.org/10.1021/ie049928g>
- [25] S. Hernández, I. R. Gudiño-Mares, J. C. Cárdenas, J. G. Segovia-Hernández, V. Rico-Ramírez, *Ind. Eng. Chem. Res.* **2005**, *44* (15), 5857–5863. DOI: <https://doi.org/10.1021/ie050169r>
- [26] J. A. Caballero, J. A. Reyes-Labarta, *Comp. Aided Chem. Eng.* **2016**, *38*, 355–360. DOI: <https://doi.org/10.1016/B978-0-444-63428-3.50064-3>
- [27] C. Adiche, B. Ait Aissa, *Chem. Eng. Res. Des.* **2016**, *109*, 150–170. DOI: <https://doi.org/10.1016/j.cherd.2016.01.015>
- [28] J. A. Caballero, I. E. Grossmann, in *Distillation Fundamentals and Principles* (Eds.: A. Górak, E. Sorensen), Elsevier, London **2014**.
- [29] M. Errico, P. Pirellas, C. E. Torres-Ortega, B. G. Rong, J. G. Segovia-Hernandez, *Chem. Eng. Process. Process Intensif.* **2014**, *85*, 69–76. DOI: <https://doi.org/10.1016/j.cep.2014.08.005>
- [30] H. Lau, J. Alvarez, K. F. Jensen, *AIChE J.* **1985**, *31* (3), 427–439. DOI: <https://doi.org/10.1002/aic.690310310>
- [31] B. W. Bequette, T. F. Edgar, *Comput. Chem. Eng.* **1989**, *13*, 641–650. DOI: [https://doi.org/10.1016/0098-1354\(89\)80003-1](https://doi.org/10.1016/0098-1354(89)80003-1)
- [32] R. Murrieta-Dueñas, R. Gutiérrez-Guerra, J. G. Segovia-Hernández, S. Hernández, *Chem. Eng. Res. Des.* **2011**, *89* (11), 2215–2227. DOI: <https://doi.org/10.1016/j.cherd.2011.02.021>
- [33] F. I. Gómez-Castro, J. G. Segovia-Hernández, S. Hernández, C. Gutiérrez-Antonio, A. Briones-Ramírez, *Chem. Eng. Technol.* **2008**, *31* (6), 1246–1260.
- [34] M. Hovd, R. D. Braatz, S. Skogestad, *Automatica* **1997**, *33* (3), 433–439. DOI: [https://doi.org/10.1016/S0005-1098\(96\)00167-7](https://doi.org/10.1016/S0005-1098(96)00167-7)
- [35] M. F. Sägfors, K. V. Waller, *IFAC Proc. Vol.* **1995**, *28* (9), 327–332. DOI: [https://doi.org/10.1016/S1474-6670\(17\)47058-3](https://doi.org/10.1016/S1474-6670(17)47058-3)
- [36] C. Moore, in *Proc. of the 1986 American Control Conf.* (Ed: E. Stear), IEEE, Piscataway, NJ **1986**, 643–650.
- [37] S. Skogestad, *Chem. Eng. Res. Des.* **2007**, *85* (A1), 13–23. DOI: <https://doi.org/10.1205/cherd06133>
- [38] J. G. Segovia-Hernández, A. Bonilla-Petriciolet, L. I. Salcedo-Estrada, *Korean J. Chem. Eng.* **2006**, *23* (5), 689–698. DOI: <https://doi.org/10.1007/BF02705913>
- [39] J. Cabrera-Ruiz, M. A. Santaella, J. R. Alcántara-Ávila, J. G. Segovia-Hernández, S. Hernández, *Chem. Eng. Res. Des.* **2016**, *123*, 165–179. DOI: <https://doi.org/10.1016/j.cherd.2017.05.006>
- [40] W. L. Luyben, *Practical Distillation Control*, Springer Science & Business Media, Heidelberg **2012**.
- [41] G. Stephanopoulos, *Chemical Process Control: An Introduction to Theory and Practice*, Prentice Hall, Englewood Cliffs, NJ **1984**.
- [42] K. Häggblom, K. Waller, in *Practical Distillation Control* (Ed.: W.L. Luyben), Van Nostrand Reinhold, New York **1992**.
- [43] A. Jiménez, S. Hernández, F. Montoy, M. Zavala, *Ind. Eng. Chem. Res.* **2001**, *40*, 3757–3761. DOI: <https://doi.org/10.1021/ie000047t>
- [44] J. G. Segovia-Hernández, S. Hernández, R. Femat, A. Jiménez, *Ind. Eng. Chem. Res.* **2007**, *46*, 546–558. DOI: <https://doi.org/10.1021/ie060438t>
- [45] G. Kaibel, M. Stroezel, *EP 0 780 147 A2*, **1996**.
- [46] A. M. Zavala-Guzmán, H. Hernández-Escoto, S. Hernández, F. O. Barroso-Muñoz, J. G. Segovia-Hernández, *Chem. Eng. Technol.* **2016**, *39*, 2238–2250. DOI: <https://doi.org/10.1002/ceat.201500601>
- [47] J. G. Segovia-Hernández, S. Hernández, V. Rico-Ramírez, A. Jiménez, *Comput. Chem. Eng.* **2004**, *28*, 811–819. DOI: <https://doi.org/10.1016/j.compchemeng.2004.02.019>